Electronic Supplementary Material (ESI) for Nanoscale.

# Supporting Information

## Enhanced Photocatalytic Hydrogen Evolution from In-situ Formation of Few-layered $MoS_2$/CdS Nanosheets Van der Waals Heterostructures

Shahid Iqbal, Ziwei Pan and Kebin Zhou*

School of Chemistry and Chemical Engineering, University of Chinese Academy of Sciences, Beijing 100049, P.R. China

*Corresponding author: kbzhou@ucas.ac.cn

### Experimental

**Preparation of ultrathin CdS NSs:** CdS NSs were synthesized through a solvothermal method as in previous research.[1] 1.0 mmol $Cd(Ac)_2.2H_2O$ and 3.0 mmol $SC(NH_2)_2$ were dispersed in 30 mL ethylenediamine (EDA) and then transferred to a Teflon-line stainless steel autoclave (50 mL), which was later maintained at 100 $^oC$ for 8 h and then naturally cooled to room temperature. After that, the bright yellow product was obtained by centrifugation and washed several times with deionized water and ethanol to remove the organic solvent, and then dried at 60 $^oC$ for 10 h.

**Preparation of $MoS_2$ NCs:** $MoS_2$ NCs were fabricated through a hydrothermal technique similar to the report in the literature. 1.0 mmol $Na_2MoO_4$ .$2H_2O$, 9.0 mmol $SC(NH_2)_2$ and 2.4 mL ammonia solution (pH=11) were dissolved in 30 mL of deionized water. After being stirred for one hour, the suspension was put into a 50 mL Teflon-lined stainless steel autoclave and heated at 220 °C for 24 h. Finally, the black solid was obtained by centrifugation and washed several times with deionized water and drying in an oven at 60 °C for 10h.

**Photocatalytic hydrogen production and in-situ formation of few-layered $MoS_2$/CdS nanosheets vdWHs.** The photocatalytic hydrogen production experiments were performed in a 250 mL Pyrex reactor attached to a close air-free gas-circulating system with constant stirring (400 rpm) at ambient temperature using 300 W Xe arc lamp (PLS-SXE300, Beijing Trusttech Co. Ltd.) coupled with a UV-cut off filter (≥420 nm). Approximately10 mg physical mixture of $MoS_2$ NCs and CdS NSs was suspended with sonication in 110 mL ethanol-water mixture (20 vol. %), and then thoroughly degassed to remove air (anaerobic conditions). The pH value was adjusted to 14.8 to guarantee sufficient hole consumption.[2] The photocatalytic $H_2$ formation rate was analyzed using an online SP-6890 gas chromatograph (GC, TCD detector, 5 $A^{\circ}$ molecular sieve columns and Argon carrier). Finally, the dark yellow product was obtained by centrifugation, washed with deionized water until of pH 7 and ethanol for three times, and then dried under vacuum conditions at 60 °C for 10h.

Apparent quantum yield (Ø) for $H_2$ formation was measured by the similar method, just applying a Xe lamp (300 W) with 420 band pass filter as the monochromic irradiation light. The total intensity of the monochromic light was estimated by averaging 5 points of the irradiation area. The Ø was calculated using the following equation:

$$\emptyset(\%) = \frac{n_{e^-}}{n_p} \times 100 = \frac{2n_{H_2}}{n_p} \times 100$$

$$n_p = \frac{\theta}{h\nu} = \frac{\mathrm{I} \times t \times A}{h\nu}$$

where Ø is the apparent quantum yield, $n_{e^-}$ is the number of reacted electrons, $n_p$ is the number of incident photos, $n_{H_2}$ is the number of evolved $H_2$ molecules, θ is the total energy (J) of incident photons, h is the Planck constant ($Js^{-1}$), ν is the frequency of photo (Hz), I is the illumination intensity ($mW/cm^2$) determined with a CEL-NP 2000 spectroradiometer, t is irradiation time (s), A is the irradiation area ($cm^2$).

## Characterizations

The XRD spectra were recorded on Philips X'Pert Pro Super diffractometer equipped with graphite-monochromatized Cu-Ka radiation (λ = 1.54178 Å). TEM analysis was conducted on H-7650 (Hitachi, Japan) operating at an acceleration voltage of 100 kV. HRTEM observations were performed on JEOL-2010 operating at an acceleration voltage of 200 kV. XPS experiments were conducted on ESCA Lab220i-XL spectrometer (VG Scientific) equipped with Al Kα radiation in twin anode at 14 kV × 16 Ma, calibrated by using the containment carbon (C 1s 284.6 eV). The steady-state UV-vis absorption spectra were recorded on a Perkin-Elmer Lambda 950 spectrophotometer. Steady-state photoluminescence (PL) spectra were conducted by a fluoromax-4 spectrofluorometer (Horiba scientific Japan). Time-resolved PL spectroscopy was carried out by time-correlated single photon counting (TCSPC) at room temperature on an F900 Steady/Transient State fluorescence spectrometer (Edinburgh Instruments, UK). The laser activates at 375 nm with a 2.5 MHz repetition rate. Mott-Schottky (MS) plots and transient photocurrent response measurements were obtained with a CHI 602 Electrochemical Work Station (Shanghai Chenhua Instrument Co. Ltd, Shanghai, China) in a standard three-electrode system at room temperature with the photocatalyst-coated FTO as the working electrode, an Ag/AgCl as a reference electrode, and Pt wire as the counter electrode.

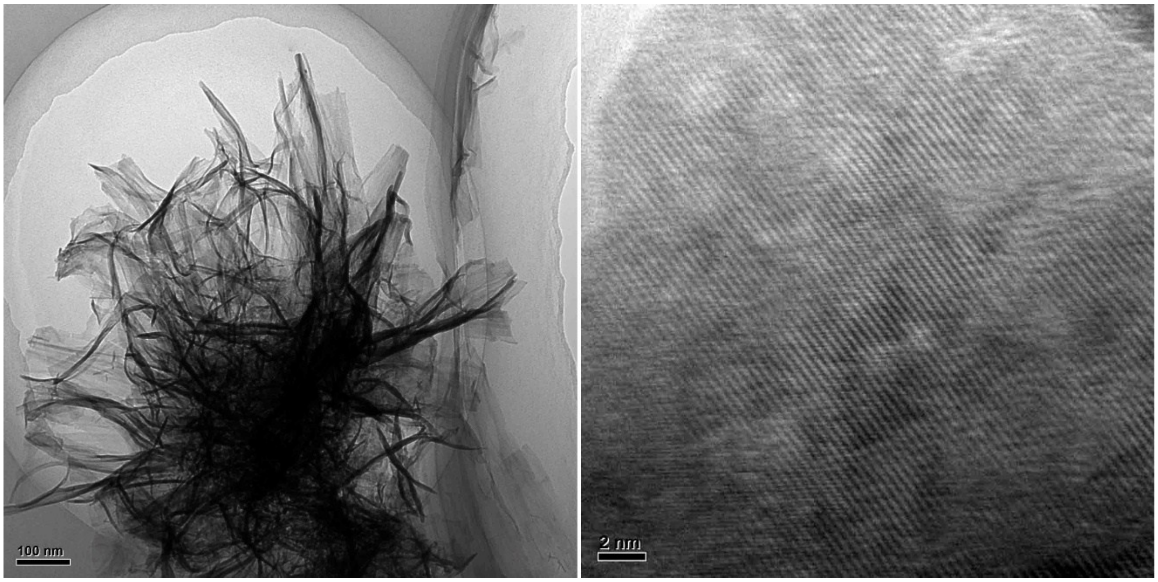

**Figure S1.** TEM and HRTEM images of as-prepared CdS nanosheets (NSs).

**Figure S2.** TEM image of as-prepared $MoS_2$ nanocrystals (NCs).

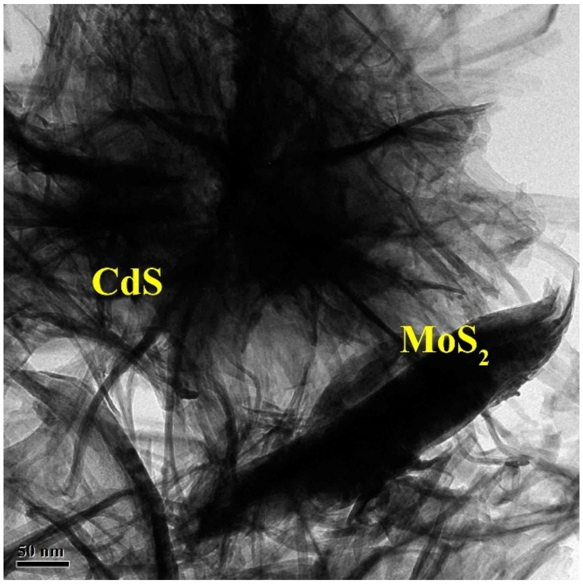

**Figure S3.** TEM image of the mixture of CdS NSs and $MoS_2$ NCs before illumination.

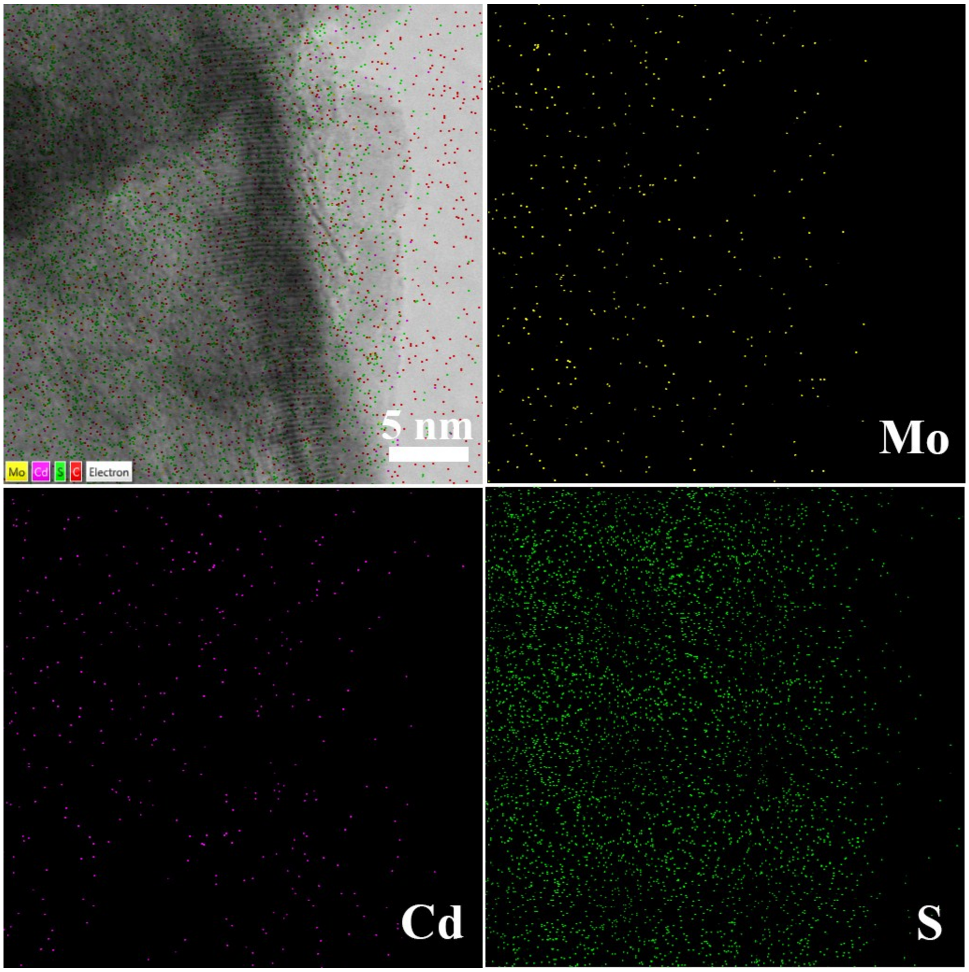

**Figure S4.** Elemental mapping of few-layered vdWHs of $MoS_2$/CdS after 10 h illumination.

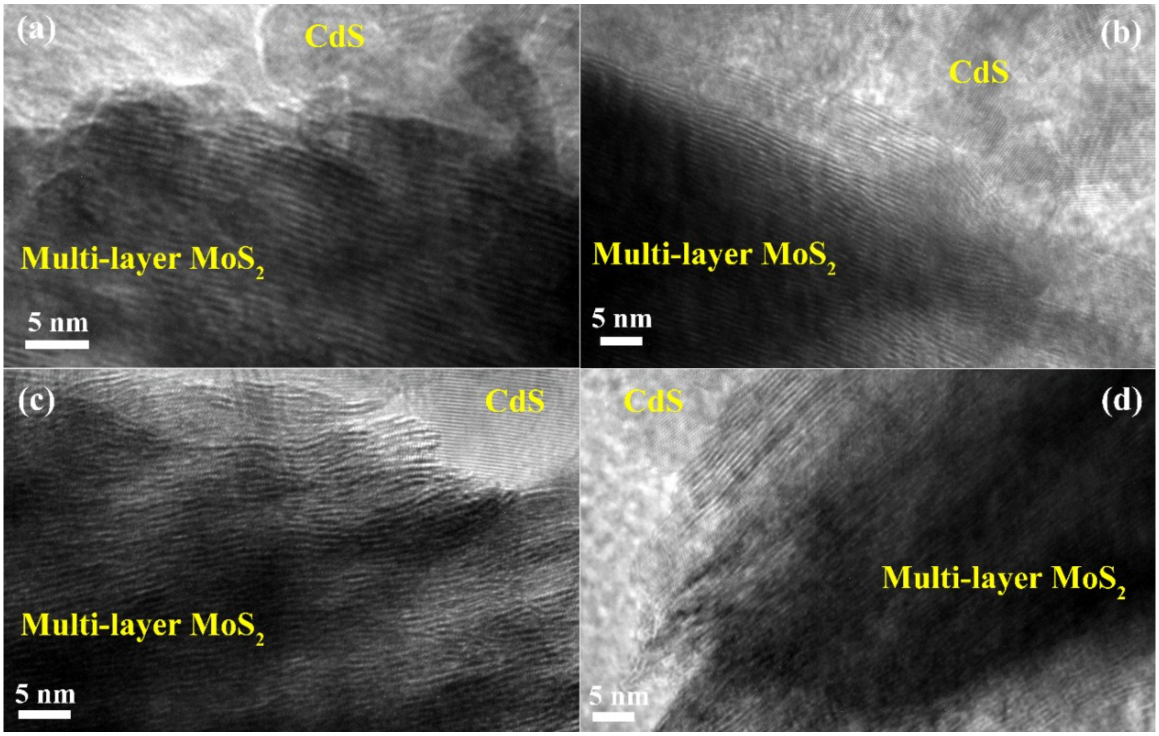

**Figure S5.** HRTEM images of $MoS_2$/CdS after different illumination times (a) 0.5 h, (b) 1 h, (c) 2 h and (d) 10 h under low-vacuum conditions (pressure, ca. 50 kPa).

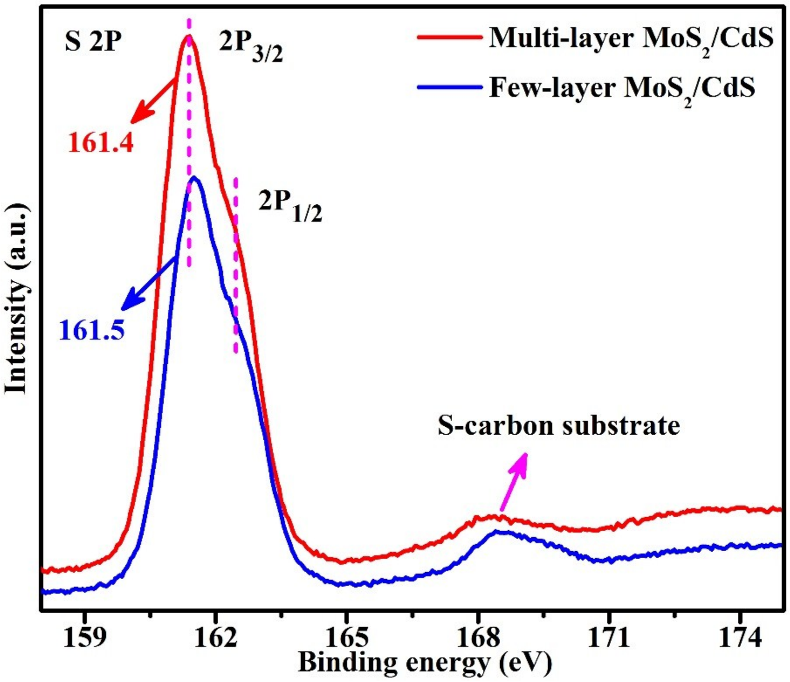

**Figure S6.** High resolution XPS spectra of S 2p in multi-layered and few-layered $MoS_2$/CdS NSs.

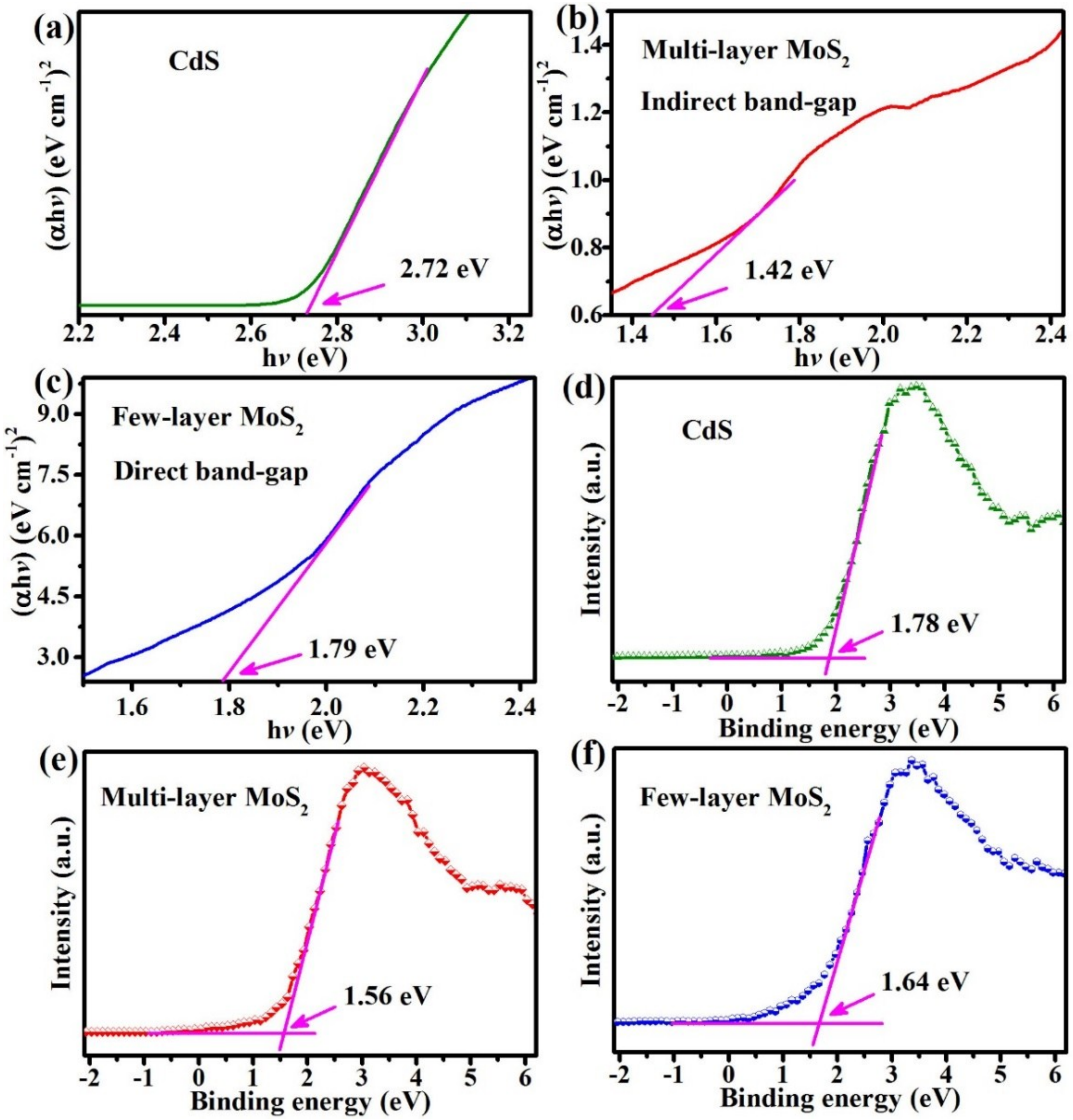

**Figure S7.** The calculated optical band-gaps of (a) CdS, (b) multi-layered $MoS_2$ (indirect band gap) and (c) few-layered $MoS_2$ (direct band gap). Valence-band XPS spectra of (d) CdS, (e) multi-layered $MoS_2$ and (f) few-layered $MoS_2$.

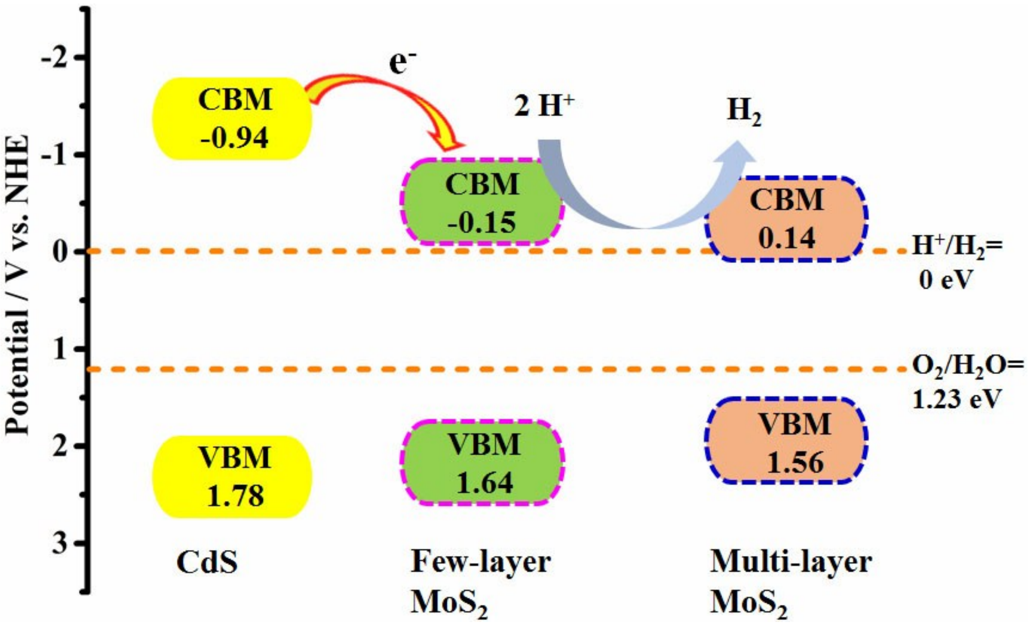

**Figure S8.** The band gap schematic of $MoS_2$/CdS heterostructure photocatalyst under visible light irradiation (λ> 420 nm).

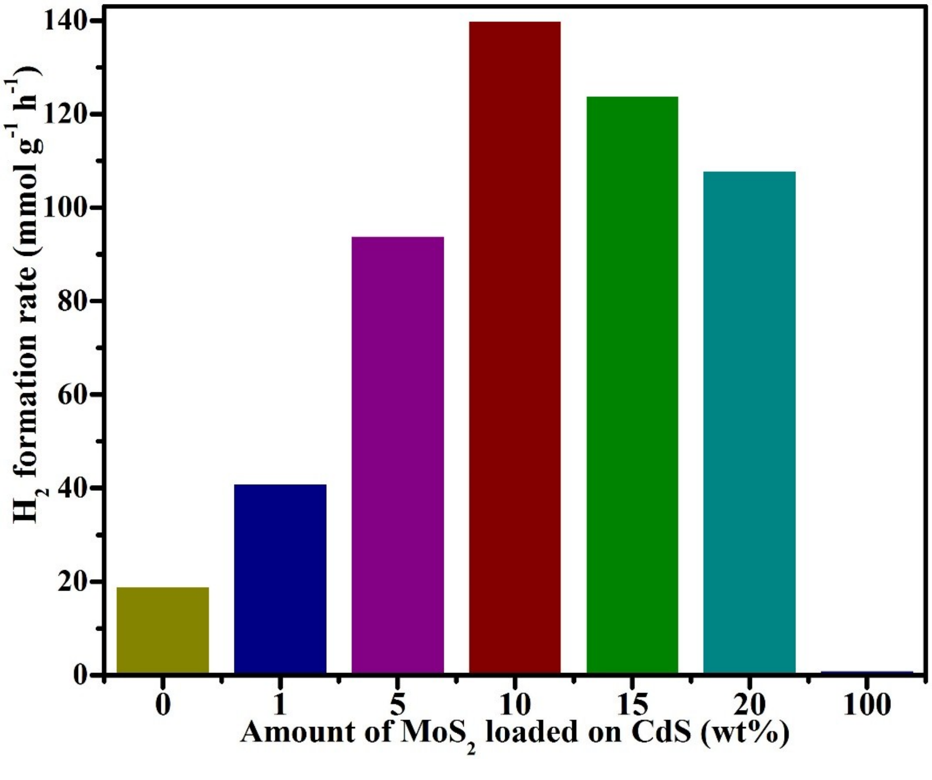

**Figure S9.** The rate of $H_2$ evolution on $MoS_2$/CdS NSs photocatalysts loaded with different amounts of $MoS_2$ under visible light irradiation (λ> 420 nm).

To investigate the effect of the amount of MoS$_2$ cocatalyst on the photocatalytic hydrogen generation, a series of the MoS$_2$/CdS heterostructures with different contents of cocatalyst was studied, as shown in Figure S9. It is found that the vdWHs have improvement H$_2$ evolution activity with the increasing amount of MoS$_2$. When the MoS$_2$ cocatalyst content is 10 wt%, the photocatalytic hydrogen production performance of MoS$_2$/CdS heterostructures reached to the highest value. The enhanced photocatalytic H$_2$ production activity upon loading of MoS$_2$ is the result of an efficient electron transfer from CdS NSs to MoS$_2$. However, higher content of MoS$_2$ leads to a decreasing H$_2$ evolution rate, which probably because an excessive amount of MoS$_2$ in the reaction system that could shield the incident light.

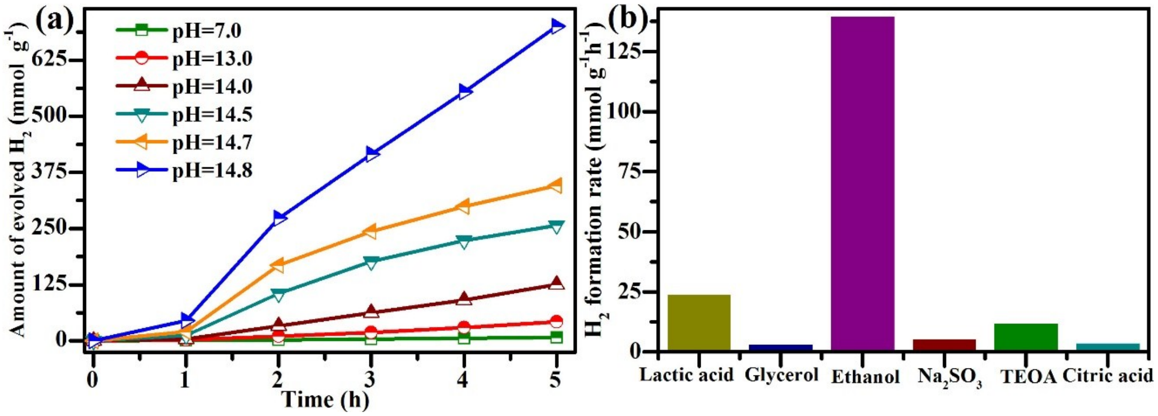

**Figure S10.** (a) The photocatalytic H$_2$ generation performance of vdWHs under different pH conditions. (b) Comparison of H$_2$ evolution rates for several sacrificial agents. The concentration was 0.1M for sodium sulfite (Na$_2$SO$_3$) and citric acid, and 20 vol. % for lactic acid, glycerol, ethanol, and triethanolamine (TEOA).

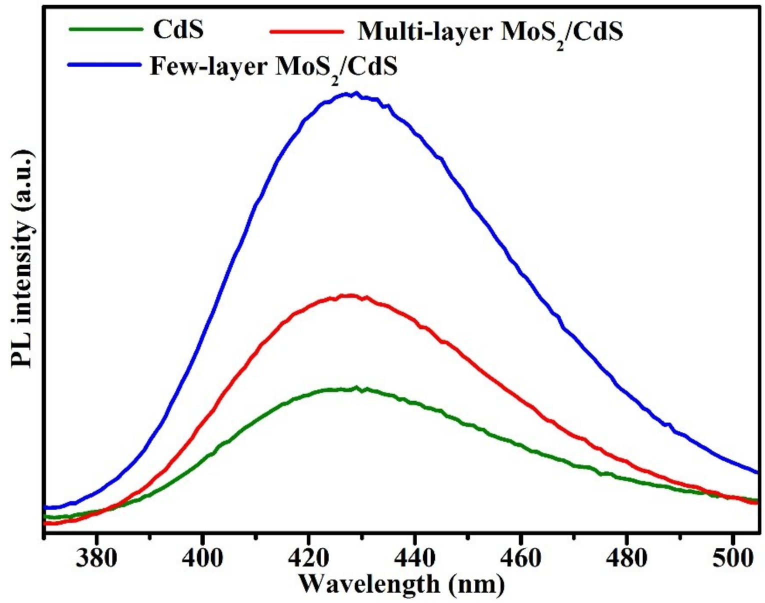

**Figure S11.** Comparison of $^{\bullet}$OH formation probed by PL spectra of 2-hydroxyterephthalic acid (product of the reaction of the $^{\bullet}$OH with terephthalic acid) taken after 30 minutes stirred in dark at an excitation wavelength of 320 nm.

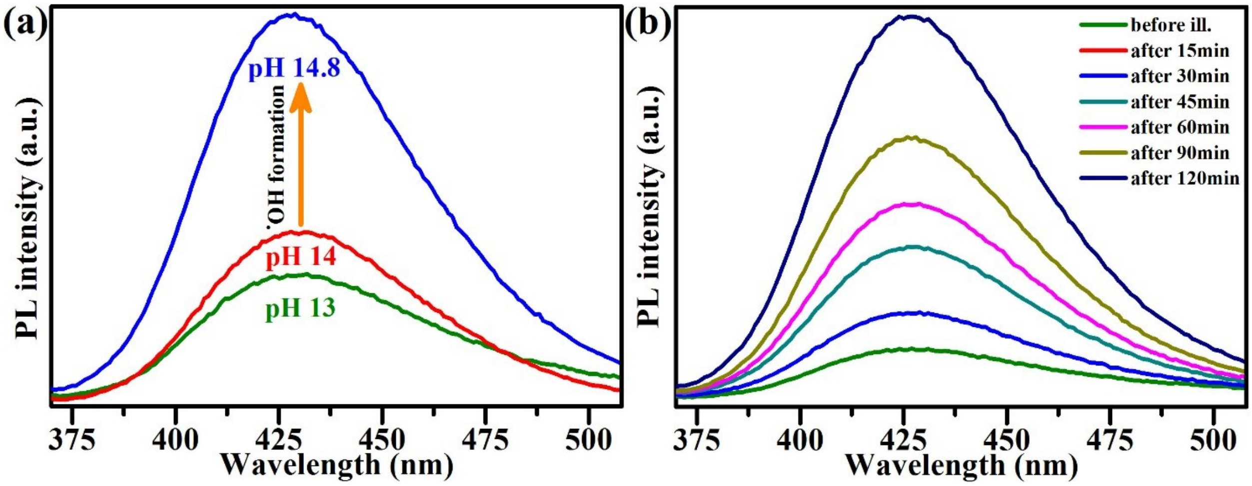

**Figure S12.** (a) Comparison of $^{\bullet}$OH formation in the few-layered $MoS_2$/CdS vdWHs probed by PL spectra of 2-hydroxyterephthalic acid (product of the reaction of the $^{\bullet}$OH with terephthalic acid) taken after 30 minutes stirred in dark under different pH conditions. (b) Increasing PL peak at 428 nm demonstrates the accumulation of the product of the reaction of terephtalic acid with the hydroxyl radical at an excitation wavelength of 320 nm.

To gain further support evidence for the proposed mechanism of the photocatalysis was provided by fluorescence technique using terephthalic acid (TA) as a probe reagent. Detection of $^{\bullet}$OH radicals in photocatalytic experiments has been carried out via reaction of TA with $^{\bullet}$OH and produced a highly fluorescent product: 2-hydroxyterephthalic acid (TAOH), which characterized by PL.[2] As shown in Fig. S10, the concentration of $^{\bullet}$OH radicals is remarkably increased in the few-layered $MoS_2$/CdS vdWHs compared to pure CdS NSs and multi-layered $MoS_2$/CdS heterostructures. Thus, the few-layered vdWHs fabricated via in-situ has a noteworthy effect on the photocatalysis activity. Fig. S11a shows that at high pH significantly more of the radicals are formed, correlating with the photocatalytic production of $H_2$ (Figure S9a). We found an increasing PL peak intensity at 428 nm (Fig. S11b) corresponding the continuous production of $^{\bullet}$OH and accumulation of the fluorescent TAOH at pH 14.8 in the few-layered $MoS_2$/CdS vdWHs. PL peak intensity at 428 nm (Fig. S11b) corresponding the continuous production of $^{\bullet}$OH and accumulation of the fluorescent TAOH at pH 14.8 in the few-layered $MoS_2$/CdS vdWHs.

Furthermore, the reducing power of few-layered $MoS_2$/CdS vdWHs was probed by using organic electron acceptors $MV^{2+}$ and $DQ^{2+}$ (where $MV^{2+}$ is dimethyl-4,4′- bipyridinium and $DQ^{2+}$ is 7,8-dihydro-2,12-dimethyl-6H-dipyrido[1,2-a:2',1'-c][1,4]diazepinediium dibromide ). As shown in Figure S12a, when an aqueous solution of few-layered $MoS_2$/CdS NSs ($1.5 \times 10^{-4}$ M) was irradiated in the presence of $MV^{2+}$ ($2.25 \times 10^{-4}$ M) under $N_2$ for 5 min, a color change from yellow to blue (inset in Figure S12a) revealed the formation of reduced cation radicals ($MV^{+\bullet}$). $DQ^{2+}$ diquat acceptor was also used as the electron acceptor for irradiation and its reduction potential [-0.7 V vs. normal hydrogen electrode (NHE)] is more negative than that of $MV^{2+}$ (-0.44 V vs. NHE).[3] As illustrated in Figure S12b, a similar result was obtained by using a diquat acceptor $DQ^{2+}$, as indicated by the green color (inset in Figure S12b) of the $DQ^{+\bullet}$. The above result for $DQ^{2+}$ suggests that the conduction band electron from few-layered $MoS_2$/CdS vdWHs must be more negative than -0.7 V vs. NHE and thus the excited state is sufficiently reducing for $H^+$ reduction.

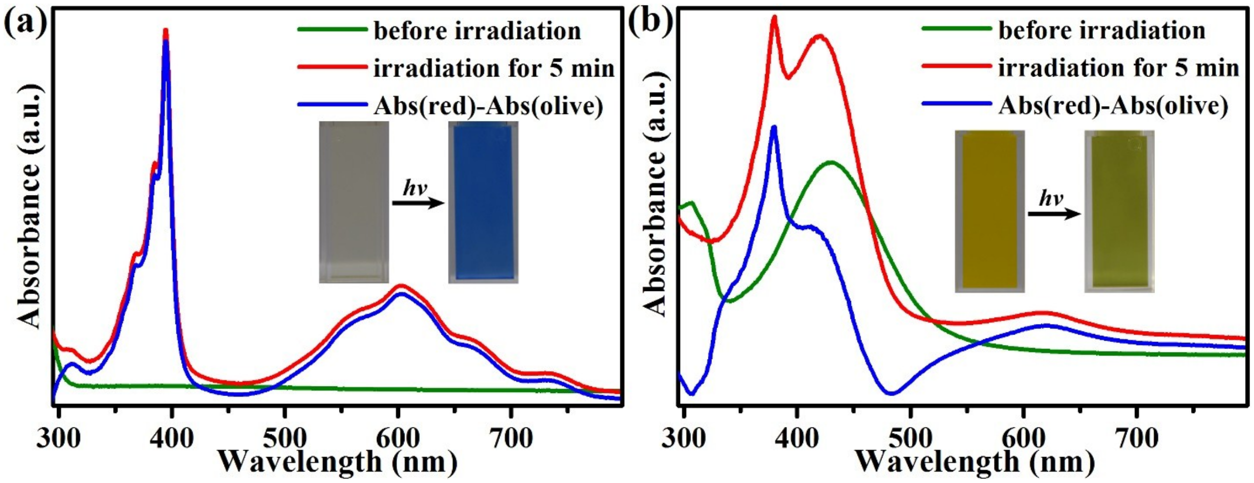

**Figure S13.** (a) Absorption spectra of 4 mL aqueous solution containing few-layered $MoS_2$/CdS NSs ($1.5 \times 10^{-4}$ M) and $MV^{2+}$ ($2.25 \times 10^{-4}$ M) before irradiation (olive line), and after irradiation ($\lambda > 420$ nm) for 5 min under $N_2$ (red line). The difference of red and olive spectra gives the absorption spectrum of the reduced $MV^{2+}$ (blue). The inset image shows the color change from light yellow to blue under visible light irradiation ($\lambda > 420$ nm). (b) Absorption spectra of 4 mL aqueous solution containing few-layered $MoS_2$/CdS NSs ($1.5 \times 10^{-4}$ M) and $DQ^{2+}$ ($2.25 \times 10^{-4}$ M) before irradiation (olive line), and after irradiation ($\lambda > 420$ nm) for 5 min under $N_2$ (red line). The difference of red and olive spectra gives the absorption spectrum of the reduced $DQ^{2+}$ (blue). The inset image shows the color change from dark yellow to green under visible light irradiation ($\lambda > 420$ nm).

**Table S1** The few-layered $MoS_2$/CdS NSs system compares favorably with other $MoS_2$/CdS photocatalysts reported in the literature in terms of hydrogen evolution ability.

| Catalyst | Scavenger | Light source | $H_2$ evolution | | Ref. |
|---|---|---|---|---|---|
| | | | Activity (mmol $h^{-1}$ $g^{-1}$) | QE (%) | |
| $MoS_2$/CdS | Lactic acid | $\lambda \geq 420$ nm (Xe) | 5.24 | 1.02 (420 nm) | 4 |
| $MoS_2$/CdS | Lactic acid | $\lambda < 420$ nm (Xe) | 0.49 | 28.5 (420 nm) | 5 |
| $MoS_2$/CdS | Lactic acid | $\lambda \geq 420$ nm (Xe) | 0.78 | 14.7 (420 nm) | 6 |
| $MoS_2$/CdS | Lactic acid | $\lambda \geq 420$ nm (Xe) | 60.28 | 50.1 (420 nm) | 7 |
| $MoS_2$/CdS | Lactic acid | $\lambda > 420$ nm (Xe) | 0.52 | 26.8 (420 nm) | 8 |
| $MoS_2$/CdS | Lactic acid | $\lambda \geq 420$ nm (Xe) | 49.8 | 41.4 (420 nm) | 9 |
| $MoS_2$/CdS | $SO_3^{2-}/S^{2-}$ | $\lambda > 420$ nm (Xe) | 2.59 | 38.4 (420 nm) | 10 |
| $MoS_2$/CdS | Lactic acid | $\lambda \geq 400$ nm (Xe) | 1.92 | 46.9 (420 nm) | 11 |
| $MoS_2$/CdS | $SO_3^{2-}/S^{2-}$ | $\lambda > 420$ nm (Xe) | 1.8 | 28.1 (420 nm) | 12 |
| $MoS_2$/CdS | Lactic acid | $\lambda > 420$ nm (Xe) | 0.54 | 7.3 (420 nm) | 13 |
| $MoS_2$/CdS | Lactic acid | $\lambda \geq 400$ nm (Xe) | 0.14 | 10.5 (450 nm) | 14 |
| $MoS_2$/CdS | Lactic acid | Simulated solar light (Xe) | 8.44 | 22.2 (420 nm) | 15 |
| $MoS_2$/CdS | Ethanol | $\lambda \geq 400$ nm (Xe) | 140 | 66.0 (420) | Present work |

## References

1. J. S. Jang, U. A. Joshi and J. S. Lee, *J. Phy. Chem. C*, 2007, **111**, 13280-13287.
2. T. Simon, N. Bouchonville, M. J. Berr, A. Vaneski, A. Adrović, D. Volbers, R. Wyrwich, M. Döblinger, A. S. Susha, A. L. Rogach, F. Jäckel, J. K. Stolarczyk and J. Feldmann, *Nat. Mater.*, 2014, **13**, 1013-1018.
3. Z. Han, F. Qiu, R. Eisenberg, P. L. Holland and T. D. Krauss, *Science*, 2012, **338**, 1321-1324.
4. X. Zhou, J. Huang, H. Zhang, H. Sun and W. Tu, *Int. J. Hydrogen Energy*, 2016, **41**, 14758-14767.
5. B. Han, S. Liu, N. Zhang, Y.-J. Xu and Z.-R. Tang, *Appl. Catal. B: Environ.,* 2017, **202**, 298-304.

6. A. Wu, C. Tian, Y. Jiao, Q. Yan, G. Yang and H. Fu, *Appl. Catal. B: Environ.*, 2017, **203**, 955-963.
7. X.-L. Yin, G.-Y. He, B. Sun, W.-J. Jiang, D.-J. Xue, A.-D. Xia, L.-J. Wan and J.-S. Hu, *Nano Energy*, 2016, **28**, 319-329.
8. M.-Q. Yang, C. Han and Y.-J. Xu, *J. Phy. Chem. C,* 2015, **119**, 27234-27246.
9. X.-L. Yin, L.-L. Li, W.-J. Jiang, Y. Zhang, X. Zhang, L.-J. Wan and J.-S. Hu, *ACS Appl. Mater. Interfaces*, 2016, **8**, 15258-15266.
10. K. Chang, M. Li, T. Wang, S. Ouyang, P. Li, L. Liu and J. Ye, *Adv. Energy Mater.*, 2015, **5**, 1402279.
11. J. He, L. Chen, F. Wang, Y. Liu, P. Chen, C.-T. Au and S.-F. Yin, *ChemSusChem*, 2016, **9**, 624-630.
12. K. Chang, Z. Mei, T. Wang, Q. Kang, S. Ouyang and J. Ye, *Acs Nano*, 2014, **8**, 7078-7087.
13. X. Zong, G. Wu, H. Yan, G. Ma, J. Shi, F. Wen, L. Wang and C. Li, *J. Phy. Chem. C,* 2010, **114**, 1963-1968.
14. J. Zhang, Z. Zhu and X. Feng, *Chem. Eur. J.*, 2014, **20**, 10632-10635.
15. K. Zhang, J. K. Kim, M. Ma, S. Y. Yim, C.-L. Lee, H. Shin and J. H. Park, *Adv. Funct. Mater.*, 2016, **26**, 4527-4534.